

Role of Intensive Milling on Microstructural and Physical Properties of Cu₈₀Fe₂₀/10CNT Nano-Composite

M. Barzegar Vishlaghi¹, A. Ataie¹

Abstract

Carbon nano-tube (CNT) reinforced metal matrix nano-composites have attracted a great deal of attention in recent years due to the outstanding physical and mechanical properties of CNTs. However, utilizing CNT as reinforcement for alloy matrixes has not been studied systematically and is still a challenging issue. In the present study, Cu₈₀Fe₂₀/10CNT nanocomposite was synthesized by mechanical alloying in two different procedures. The effects of CNT addition on microstructural and physical properties of nano-composite, Phase composition, morphology, magnetic and electrical properties of the samples were investigated by X-ray diffraction, field emission scanning electron microscopy, vibrating sample magnetometer, and four point probe techniques, respectively. The results showed that addition of CNT suppressed the solid solubility extension of Fe in Cu matrix. Dispersion and implantation of CNTs in the metal matrix improved, particles size was smaller and their shape was more granular when CNTs were added at the start of milling. Saturation magnetization and coercivity of composite samples increased with addition of CNT probably due to the presence of non-dissolved Fe in nano-composites and inhomogeneity of microstructure, respectively. Electrical resistivity of nano-composites was higher than that of matrix alloy. The increment was more when milling time of CNTs and metal powder was shorter.

Keywords: Carbon nanotube; Mechanical milling; Metal matrix composite; Physical properties

1. Introduction

The interest on utilizing CNT as reinforcement in metal matrix composites has grown significantly in recent years [1-4] due to outstanding mechanical properties, high electrical and thermal conductivity, and chemical inertness of CNTs [5, 6]. But the difficulty of dispersion of CNTs in matrix and poor wettability of CNT with metals such as copper [7] are drawbacks in synthesizing CNT-metal composites. Earlier studies proved that mechanical alloying is an effective method for dispersion of CNTs in metal matrix [3, 8]. A few researches have been done recently on the effect of different parameters such as morphology of CNT [4] and metal particles [8] on properties of aluminum and copper matrix composites using mechanical alloying. But no systematic study has been carried out on metastable copper alloys reinforced with CNTs. Among binary Cu-based metastable alloys, Cu-Fe alloys have attracted a lot of interest due to their outstanding magnetic

properties [9-11], high strength and high electrical conductivity [12] and lower price of Fe compared to other metals such as W, Nb, V, and Ag [13]. Mechanical alloying can extend the solid solubility of immiscible elements in binary systems [14, 15]. Limits of solubility of Fe in Cu change considerably in alloying systems with various milling conditions. Lots of studies have been focused on Cu-Fe alloying system with various compositions and showed that the different structures were obtained for various compositions. For example Eckert et al. synthesized nano-crystalline Fe_xCu_{1-x} powders with a wide range of composition and showed that single phase fcc alloys and single phase bcc alloys are formed with $x < 60$ and with $x > 80$, respectively after 24 h milling. For $60 < x < 80$ both fcc and bcc phases coexist [16].

Furthermore, Gaffet et al. and Majumdar et al. have reported that bcc Fe-Cu solid solution formation is restricted to 0-20 wt. % Cu after milling for longer time [17, 18]. In this work,

1- School of Metallurgy and Materials Engineering, College of Engineering, University of Tehran, Tehran, Iran.

the effect of CNT and the milling duration of metal powder with CNT on morphology and physical properties of $\text{Cu}_{80}\text{Fe}_{20}/10\text{CNT}$ nano-composite were investigated.

2. Experimental

Starting materials were commercially pure Cu and Fe powders (99%, $<150\ \mu\text{m}$), and multi-walled carbon nano-tubes (with average diameter of 20-30 nm and several micrometers in length and a purity more than 85%). Multi-walled carbon nano-tube (MWCNT) used in this work was synthesized by catalytic chemical vapor deposition method at Tehran Research Institute of Petroleum Industry. TEM image of as-received CNT is shown in Fig.1. CNTs were sonicated in acetone for 20 min for removing their tangles. In order to produce $\text{Cu}_{20\text{wt}\%}\text{Fe}-10\text{wt}\%\text{CNT}$ nano-composite, proper amount of starting materials were mixed and milled in two different procedures: 1) Composite C1: Cu and Fe powders were milled for 10 h and then CNTs were added to the mixed powder and milled for 5 h. In this procedure, sampling was carried out after 1, 3 and 5 h of milling after addition of CNT and the related samples were labeled as C1-1, C1-3, and C1-5, respectively. 2) Composite C2: a mixture of Cu, Fe and CNTs were milled for 15 h. Proper weight proportions of Cu and Fe powders were also milled for 10 and 15 h to produce $\text{Cu}_{80}\text{Fe}_{20}$ alloy in order to compare with nano-composite samples. All alloying and mixing processes were carried out in a

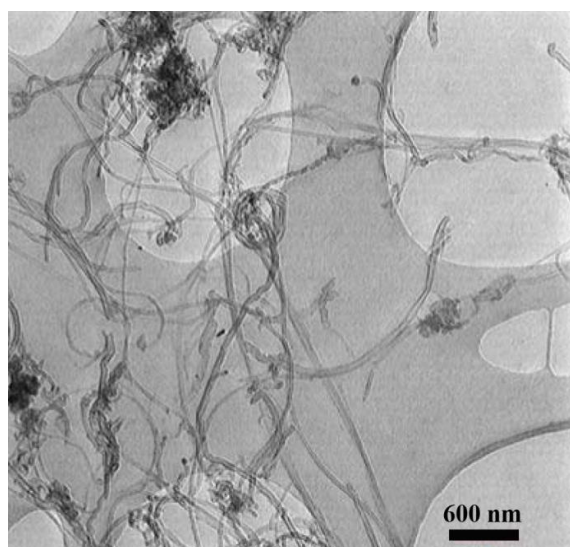


Fig. 1. TEM image of as-received CNTs.

planetary ball mill with hardened chromium steel vial and balls under argon atmosphere. Ball to powder weight ratio and milling speed were 20:1 and 300 rpm, respectively. Phase composition was studied by XRD using a Philips PW-3710 diffractometer with a $\text{Cu K}\alpha$ radiation. XRD peak broadening using Williamson-Hall approximation was applied to determine mean crystallite size of the milled powders [19]. Morphology of milling products was studied by Hitachi S4160 scanning electron microscope (SEM). For higher magnification, field emission scanning electron microscope (FESEM) was employed. Magnetic properties of the samples were investigated using vibrating sample magnetometer (VSM) apparatus under the maximum magnetic field of 10 kOe. Sample powders were cold pressed under the pressure of 50 MPa for electrical resistivity measurement which was carried out by four point probe technique.

3. Result and Discussion

XRD patterns of nano-composite samples together with 10 and 15 h milled $\text{Cu}_{80}\text{Fe}_{20}$ alloys are shown in Fig. 2. As can be seen, only Cu peaks are discernable in 10 and 15 h milled $\text{Cu}_{80}\text{Fe}_{20}$ alloys, which means that Fe is completely dissolved in Cu. However, a small peak of Fe is discernable in XRD patterns of nano-composites which are related to non-dissolved Fe phase. It indicates that CNTs not only suppressed the dissolution of Fe in Cu when they were added at the start of milling,

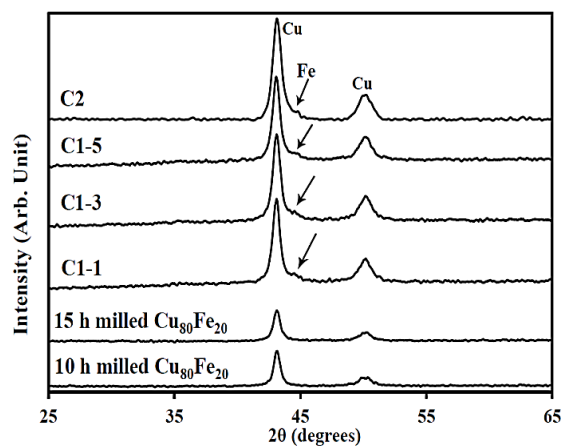


Fig. 2. XRD patterns of nano-composite samples together with 10 and 15 h milled $\text{Cu}_{80}\text{Fe}_{20}$ alloys.

but also expelled Fe atoms from Cu lattice when they were added at late stages of the milling. This phenomenon could be explained by various reasons. First, CNTs decrease the milling energy due to their lubricating nature, which result in decreasing the driving force for the formation of extended solid solution. Reduction of milling energy is confirmed by larger crystallite size [20] of nano-composites compared with that of $\text{Cu}_{80}\text{Fe}_{20}$ alloys, as shown in Table 1, and higher intensity of peaks in XRD patterns of nano-composites (Fig. 2). There is also no considerable change in crystallite size of C1-1, C1-3 and C1-5 samples (Table 1), which indicates that milling energy did not increase further after addition of CNT. Second is the dissolution of carbon atoms from damaged CNTs in Cu [3] resulting to precipitation of Fe atoms. As can be seen in Table 1, lattice parameter of nano-composites are smaller than that of $\text{Cu}_{80}\text{Fe}_{20}$ alloys which can be related to the expulsion of Fe atoms from Cu lattice [21]. Carbon atoms also obstruct the diffusion paths and make the penetration of Fe in Cu lattice more difficult. Third, reduction of possible surface oxides in powder by carbon atoms could result in more pure iron in powder mixtures. Fourth reason could be the local temperature rise during milling [20] which might result in precipitation of dissolved Fe. It is also noted that reflections of carbides and CNT were not detected in XRD patterns of nano-composites. The latter indicates well dispersion and embedment of CNTs in Cu matrix and the strains induced by

ball milling on CNTs, which reduces the peak intensity. As can be seen in Table 1, mean crystallite size of C2 sample is about 46 nm which is larger than that of C1-5 sample (34 nm), while both were milled for 15 h. Therefore, it is assumed that milling energy was lower when CNTs were added at the start of the milling.

SEM images of C1-5 and C2 nano-composite samples are shown in Figs. 3a and 3b, respectively. It can be seen that particles are slightly larger in C1-5 sample compared with C2 sample. It is well known that cold welding of particles and fracturing are two competing processes during mechanical milling [20]. Previous studies showed that in Al-CNT composite, mean particle size first increased and then began to decrease after milling for 6 h. Thus, it is possible for C1-5 nano-composite that small flakes start to form after CNT addition and milling for 5 h. the

Table 1. Mean crystallite size and lattice parameter of nano-composites and $\text{Cu}_{80}\text{Fe}_{20}$ alloys

Sample	Mean crystallite size (nm)	Lattice parameter (nm)
C1-1	35	0.36239
C1-3	35	0.36235
C1-5	34	0.36251
C2	46	0.36266
15 h milled $\text{Cu}_{80}\text{Fe}_{20}$	19	0.36284
10 h milled $\text{Cu}_{80}\text{Fe}_{20}$	23	0.36283

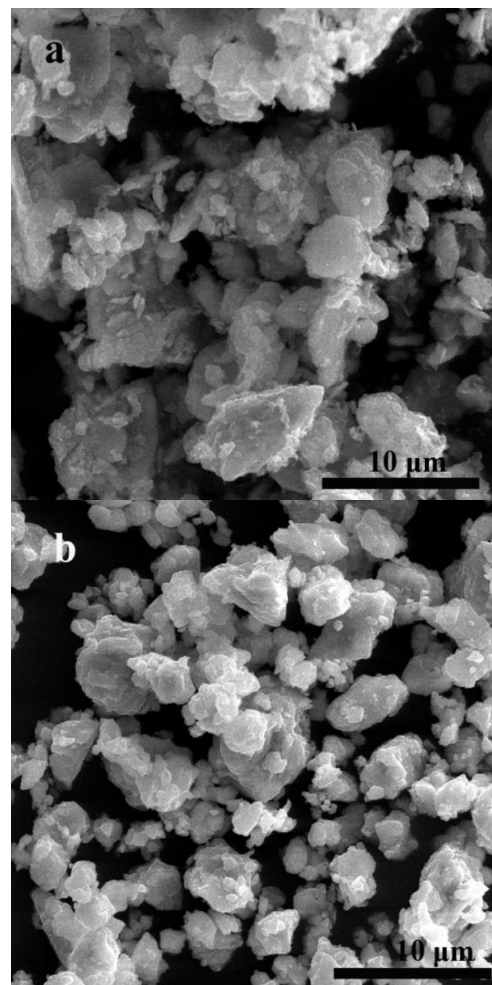


Fig. 3. SEM images (a) C1-5 and (b) C2 nano-composites.

same result was also reported for Cu-CNT composite [22]. Large amount of CNTs entrapped between particles and decreased the cold welding between them. For prolonged milling times (as in C2 nano-composite), CNTs implant into the metal particles, cold welding and fracturing of particles reach equilibrium, and particles shape become more granular.

FESEM images of nanocomposites (Fig. 4) also confirm the above claims. CNTs are observable in C1-1 and C1-5 samples (Figs. 4a

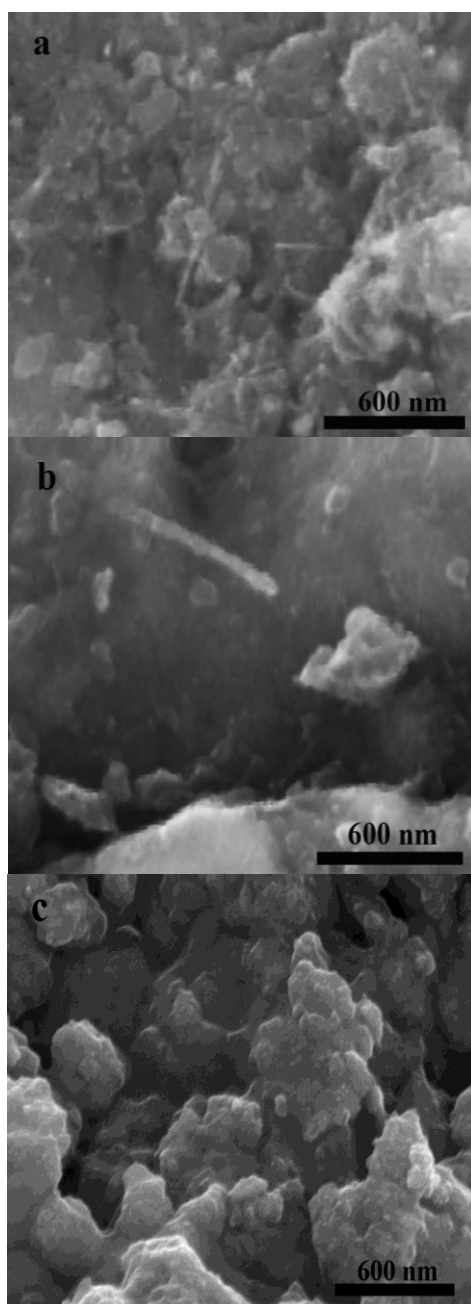


Fig. 4. FESEM images of (a) C1-1, (b) C1-5 and (d) C2 nano-composites.

and 4b respectively), but they cannot be detected in C2 sample (Fig. 4c) indicating the complete implantation of CNTs into metal particles. As can be seen in Figs. 4a and 4b, CNTs did not undergo significant damage or shortening due to the high ductility of matrix, which absorbs the impact energy during milling through the plastic deformation. It has been shown that significant breakage of CNTs occurs at initial stages of mechanical alloying. But no further changes occur in CNT length for more than 1 h of ball milling due to the embedding CNTs within ductile particles [23]. Hence, it is presumed that CNTs in C2 sample are not significantly damaged.

Hysteresis loops of samples are shown in Fig. 5 and magnetic data are listed in Table 2. It can be seen that 15 h milled $\text{Cu}_{80}\text{Fe}_{20}$ sample has a weak ferromagnetic behavior which is in agreement with previous work [21]. However, both saturation magnetization (M_s) and coercivity (H_c) of nano-composites increased by introduction of CNT. A slight decrease in M_s of C1-5 and C2 samples compared with C1-1 can be related to the possible formation of carbides or change in amount of dissolved Fe in Cu. CNTs are non-magnetic materials or very weak ferromagnetic due to the possible catalyst particles [24, 25]. Therefore, high M_s can be attributed to the non-dissolved Fe in Cu matrix. This result is correlated well with the XRD results. Increase in saturation magnetization due to the precipitation of bcc Fe was also reported in mechanically alloyed Fe-Cu system [17]. Increasing H_c might be due

Table 2. Magnetic properties of nano-composites and 15 h milled $\text{Cu}_{80}\text{Fe}_{20}$ alloy

sample	Milling time after addition of CNT (h)	M_s (emu/g)	M_r (emu/g)	H_c (Oe)
C1-1	1	10.5	2	305
C1-5	5	9.7	1.7	275
C2	15	9.4	1.5	273
15 h $\text{Cu}_{80}\text{Fe}_{20}$	-	7.10	0.03	27

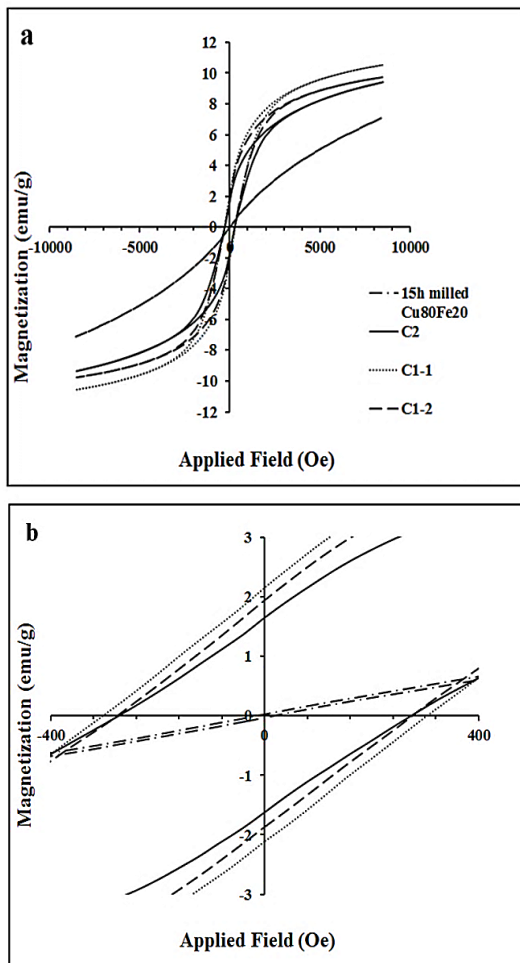


Fig. 5. (a) Hysteresis loops of samples, (b) enlarged view of loops at center.

to the exchange bias effect which could be the result of inhomogeneity of microstructure [26]. H_c decreased by increasing milling time of metal powder with CNT, because the inhomogeneity of microstructure decreased due to the better dispersion and implantation of CNTs in the matrix with increasing milling time. Electrical resistivity of cold pressed nano-composites was measured using four point probe technique. Resistivity of C1-5 is $0.52 \Omega \cdot \text{cm}$ which is more than 20 time larger than that of C2 nano-composite ($0.022 \Omega \cdot \text{cm}$). Electrical resistivity of MWCNT is of the order of $10^{-3} \Omega \cdot \text{cm}$ [6, 27] which is about the same value as 15 h milled $\text{Cu}_{80}\text{Fe}_{20}$ alloy. Increasing the electrical resistivity by introduction of CNT into the $\text{Cu}_{80}\text{Fe}_{20}$ matrix can be due to the increased porosity and low adherence between metal matrix and CNTs, because of the negligible wettability of CNT by copper and iron [7, 28]. Higher electrical

resistivity of C1-5 nano-composite can be related to the poor distribution and implantation of CNTs in matrix due to the shorter milling time, as shown by FESEM images, and higher amount of porosity.

According to the above results, the procedure which CNTs were added from the start of milling was the optimum one because of the homogeneous microstructure which leads to the uniformity of physical properties.

4. Conclusions

$\text{Cu}_{80}\text{Fe}_{20}/10\text{CNT}$ nano-composite was synthesized by two different procedures and the effect of CNT on phase composition and morphology of products were investigated.

Introduction of CNT suppressed the extension of solid solubility of Fe in Cu.

Particles were smaller in size and more regular in shape, and CNTs were completely embedded in matrix when CNTs and metal powders were milled for 15 h.

Saturation magnetization and coercivity of composite samples increased on increasing CNT content probably due to the presence of non-dissolved Fe in nano-composites and inhomogeneity of microstructure, respectively. Electrical resistivity of nano-composites was higher than that of matrix alloy. The increment was more when milling time of CNTs and metal powder was shorter.

Acknowledgment

The financial supports of this work by the University of Tehran and Iran Nanotechnology Initiative Council are gratefully acknowledged.

References

1. Taaa, Z., Geng, H., Yu, K., Yang, Z., Wang, Y., *Mater. Lett.* Vol. 58 (2004) pp.3410–3413.
2. Wang, L., Choi, H., Myoung, J., Lee, W., *Carbon* Vol. 47 (2009) pp. 3427–3433.
3. Esawi, A.M.K., Morsi, K., Sayed, A., Abdel Gawad, A., Borah, P., *Mater. Sci. Eng. A*. Vol. 508 (2009) pp. 167–173.
4. Esawi, A.M.K., Morsi, K., Sayed, A., Taher, M., Lanka, S., *Compos. Part A-Appl. S.* Vol. 42 (2011) pp. 234–243.

5. Salvétat, J.P., Bonard, J.M., Thomson, N.H., Kulik, A.J., Forro, L., Benoit, W., Zuppiroli, L., *Appl. Phys. A-Matter*. Vol. 69 (1999) pp. 255–260.
6. Cha, S.I., Kim, K.T., Lee, K.H., Mo, C.B., Jeong, Y.J., Hong, S.H., *Carbon*. Vol. 46 (2008) pp. 482-488.
7. Chu, K., Jia, C.C., Jiang, L.K., Li, W.S., *Mater. Des.* Vol. 45 (2013) pp. 407–411.
8. Uddin, S.M., Mahmud, T., Wolf, C., Glanz, C., Kolaric, I., Volkmer, C., Holler, H., Wienecke, U., Roth, S., Fecht, H.J., *Compos. Sci. Technol.* Vol. 70 (2010) pp. 2253–2257.
9. Crespo, P., Barro, M.J., Navarro, I., Viizquez, M., Hemando, A., *J. Magn. Magn. Mater.* Vol. 140 (1995) pp. 85-86.
10. Kong, L.T., Liu, B.X., *J. Alloy. Compd.* Vol. 414 (2006) pp. 36-41.
11. Gonzalez, J., Zhukova, V., Zhukov, A.P., Del Val, J.J., Blanco, J.M., Pina, E., Vazquez, M., *J. Magn. Magn. Mater.* Vol. 221 (2000) pp. 196-206.
12. Biselli, C., Morris, D.G., *Acta Mater.* Vol. 44 (1996) pp. 493-504.
13. Azabou, M., Gharsallah, H.I., Escoda, L., Sunol, J.J., Kolsi, A.W., Khitouni, M., *Powder. Technol.* Vol. 224 (2012) pp. 338-344.
14. Kravtsova, A.N., Yalovega, G.E., Soldatov, A.V., Yan, W.S., Wei, S.Q., *J. Alloy. Compd.* Vol. 469 (2009) pp. 42-49.
15. Crivello, J.C., Nobuki, T., Kuji, T., *Mater. T. JIM*. Vol. 49 (2008) pp. 521-531.
16. Eckert, J., Holzer, J.C., Johnson, W.L., *J. Appl. Phys.* Vol. 73 (1993) pp. 131-141.
17. Majumdar, B., Manivel Raja, M., Narayanasamy, A., Chattopadhyay, K., *J. Alloy. Compd.* Vol. 248 (1997) pp. 192-200.
18. Gaffet, E., Harmelin, M., Faudot, F., *J. Alloy. Compd.* Vol. 194 (1) (1993) pp. 23-30.
19. Williamson, G.K., Hall, W.H., *Acta Metall.* Vol. 1 (1953) pp. 22-31.
20. Suryanarayana, C., *Prog. Mater. Sci.* Vol. 46 (2001) pp. 1-184.
21. Mashimo, T., Huang, X., Fan, X., *Phys. Rev. B* Vol. 66 (2002) pp 132401-132404.
22. Li, H., Misra, A., Zhu, Y., Horita, Z., Koch, C.C., Holesinger, T.G., *Mater. Sci. Eng. A* Vol. 523 (2009) pp. 60–64.
23. Wu, Y., Kim, G.Y., Russell, A.M., *Mater. Sci. Eng. A* Vol. 532 (2012) pp. 558-566.
24. Kuryliszyn-Kudelska, I., Malolepszy, A., Mazurkiewicz, M., Stobinski, L., Dobrowolski, W., *Acta. Phys. Pol A*. Vol. 119 (2011) pp. 597-599.
25. Grechnev, G.E., Desnenko, V.A., Fedorchenko, A.V., Panifilov, A.S., Prylutsky, Y.I., Grybova, M.I., Matzui, L.Y., Ritter, U., Scharff, P., Kolesnichenko, Y.A., *Mat.-wiss. u. Werkstofftech.* Vol. 42 (2011) pp. 29-32.
26. Nogues, J., Sort, J., Langlais, V., Skumryev, V., Surinach, S., Munoz, J.S., Baro, M.D., *Phys. Rep.* Vol. 422 (2005) pp. 65 – 117.
27. Kaneto, K., Tsuruta, M., Sakai, G., Cho, W.Y., Ando, Y., *Met.* Vol. 103 (1999) pp. 2543-2546.
28. Yu-Feng, G., Yang, Y., De-Yan, S., *Chinese. Phys. Lett.* Vol. 28 (2011) pp. 1-4.